The final publication is available at

https://doi.org/10.1039/c7cy01231d

Additional Information

Journal Name

ARTICLE

A comprehensive mechanistic study on the visible-light photocatalytic reductive dehalogenation of haloaromatics mediated by Ru(bpy)₃Cl₂

Mireia Marin,[a] Miguel A. Miranda[a],* and M. Luisa Marin[a],*

Visible light photoredox catalysis is emerging as a versatile technique for a great variety of chemical transformations. Specifically, Ru(bpy)$_3^{2+}$ has been widely used as transition metal based photocatalyst; however little if any attention has been paid to the thermodynamic analysis of the photoredox processes that occur in the photocatalytic cycle of the studied reactions, or, even more interestingly, to the examination of the kinetic feasibility of the involved processes. In addition, only few and far between studies on the progress of the reaction have been performed. Organic halides constitute a major concern for environmental remediation since they are reluctant to aerobic oxidation. Therefore p-halonitrobenzene (X-NB) derivatives have been selected in the present work as the model compounds to get a deeper understanding on their photocatalytic reduction using visible-light and Ru(bpy)$_3^{2+}$. Thermodynamic estimations were made on the basis of the experimentally determined energy of the LUMO of Ru(bpy)$_3^{2+}$, which was determined as 54.5 kcal x mol^{-1} from the cross-point of the normalized emission and excitation spectra, and redox potentials of X-NB, and of several sacrificial amines. As anticipated from chemical intuition, the feasibility of the global photoredox process increased upon going down in the group of halogens regardless the participation of the oxidative or reductive quenching cycles. To unequivocally demonstrate the direct participation of the excited state of Ru(bpy)$_3^{2+}$ in the photoreduction, steady-state and time-resolved experiments were carried out upon increasing X-NB or amines concentration; this allowed determining the quenching rate constants for the electron transfer processes, which were found to be in the range of 10^8 M^{-1} x s^{-1} for the X-NB and 10^6 M^{-1} x s^{-1} for the amines. Therefore the main role of the oxidative quenching cycle has been demonstrated under the experimental conditions employed. A good correlation was found between the thermodynamic and kinetic parameters, in agreement with the expectations from Marcus theory. Upon optimization of the reaction conditions, reductive dehalogenation was found to occur leading to the parent nitrobenzene.

Introduction

During the past decades, visible-light photoredox catalysis has been in the focus of many investigations due to its efficiency, versatility and potential applications, which range from environmental remediation[1-6] to synthetic chemistry.[7-12] In this context, tris(2,2'-bipyridyl)ruthenium(II) chloride, (Ru(bpy)₃Cl₂), has been widely used as transition metal based photocatalyst for a great number of chemical processes.[13-22] However, the precise role of Ru(bpy)$_3^{2+}$ in such photochemical processes is often unclear, since elucidation of the operating oxidative or reductive quenching cycle is often forgotten, in spite of its

importance to optimize selection of reactants. For instance, little if any attention has been paid to the thermodynamic analysis of the photoredox processes that occur in the organometallic photocatalytic cycle of the studied reactions, and examination of kinetic feasibility of the involved processes is uncommon. In addition, only few studies on the progress of the reaction have been performed. Nevertheless, assuming that the photoredox catalytic cycle is a crucial feature in this area, further mechanistic investigation is required.

Organic halides are ubiquitous man-made compounds with many different applications as insecticides, solvents, polymers or drugs. Unfortunately, halogenated compounds are in general reluctant to aerobic oxidation, so they constitute a major concern for environmental remediation.[23-24] Chemical reduction, mediated by different metals, in which the halogen is replaced with hydrogen, has been widely reported to achieve such goal.[25] It is generally accepted that the ease for reduction increases upon going down in the group of halogens according

[a]. *Instituto de Tecnología Química, Universitat Politècnica de València-Consejo Superior de Investigaciones Científicas, Avda. de los Naranjos s/n, E-46022, Valencia, Spain. E-mails: mmiranda@qim.upv.es; marmarin@qim.upv.es*
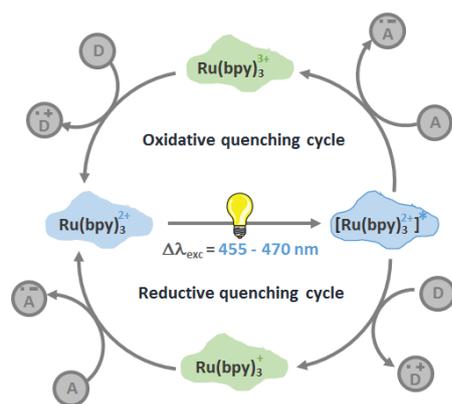
Fig. 1. Photoredox catalytic cycle of Ru(bpy)$_3$$^{2+}$ in the presence of electron acceptors (A) and electron donors (D), proceeding through the oxidative or the reductive quenching cycles.

with a decrease in the C-X bond energy. Furthermore, benzylic halides are the most easily reduced, followed by allylic, vinylic, aromatic and aliphatic.[25] With that purpose, in this manuscript we have selected Ru(bpy)$_3$$^{2+}$ as a representative photocatalyst and reduction of haloaromatics as the model reaction. Specifically, we have undertaken a systematic mechanistic study on the reduction of a family of p-halonitrobenzene derivatives (X-NB) in the presence of sacrificial amines. The global photoredox reaction could in principle operate through the oxidative or through the reductive quenching cycles as illustrated in Figure 1, in agreement with related literature precedents.[7-8, 13, 26] In the proposed photocatalytic cycle, blue light ($\Delta\lambda = 455 - 470$ nm) is selectively absorbed by Ru(bpy)$_3$$^{2+}$ leading to its excited state ([Ru(bpy)$_3$$^{2+}$]*). Then, as a result of the overall photocatalytic cycle X-NB derivatives are reduced in the presence of tertiary amines used as sacrificial electron donors.[26-27] Different aspects of this photodehalogenation have been analysed herein: thermodynamics, excited state dynamics and formation of photoproducts. Evidence supporting this reaction happening through the oxidative quenching cycle has been obtained by correlation between the kinetic and thermodynamic data. As a result, a deeper understanding of the mode of action of this paradigmatic organometallic photocatalyst has been achieved and the importance of the kinetic experimental analysis has been highlighted.

Experimental

Chemicals

Tris(2,2'-bipyridyl)dichlororuthenium (II) hexahydrate (Ru(bpy)$_3$Cl$_2$.6H$_2$O), nitrobenzene (NB), 1-fluoro-4-nitrobenzene (F-NB), 1-chloro-4-nitrobenzene (Cl-NB), 1-bromo-4-nitrobenzene (Br-NB), 1-iodo-4-nitrobenzene (I-NB), diethyl 1,4-dihydro-2,6-dimethyl-3,5-pyridinedicarboxylate (Hantzsch ester, HE), isopropanol, aniline, trimethylamine (TEA), N,N-diisopropylethylamine (DIPEA) and tetrabutylammonium hexafluorophosphate (TBA) were purchased from Sigma-Aldrich. Acetonitrile was HPLC quality from Scharlau. Milli-Q grade water was used for the HPLC analyses.

Instrumentation: Electrochemistry

Electrochemical experiments were carried out in a quartz cylindrical three electrode cell on a Versastat 3 (Princeton Applied Research) electrochemical workstation with a platinum working electrode, a platinum wire as the counter electrode and Ag/AgCl (saturated KCl) as the reference electrode.

Instrumentation: Photophysics

Absorption spectra UV-Vis were performed on a Cary 50 UV-Vis spectrophotometer (Varian). Steady-state luminescence spectra were recorded on a Photon Technology International (PTI) (LSP-220B) fluorometer equipped with a 75 W Xe lamp. Time-resolved luminescence experiments were carried out on an EasyLifeTM X fluorometer (from Optical Building Blocks Corporation) with a 460 nm excitation LED and a long-pass filter of 475 nm to filter scattering from the excitation LED in the detection system. Quartz cells of 1 cm optical path length were employed for all measurements. Steady-state and time-resolved quenching experiments were performed at 15 ºC using a cooling bath, under nitrogen, in acetonitrile-water (4:1) solutions.

Instrumentation: Photochemistry

A homemade set-up photoreactor built with 2.5 m strip blue-LEDs Samsung SMD5630 IP20 of 15 W/m, spiral-shaped and an irradiation band of $\Delta\lambda = 455 - 470$ nm was used for the photochemical reactions.

Instrumentation: HPLC Analysis

The HPLC measurements were carried out using a Waters 600 C chromatograph equipped with a Waters 600 pump and controller, a Waters in-Line degasser AF and a Waters 996 photodiode array detector. A Teknokroma C18 Mediterranea Sea (25 × 0.46 mm and 5 μm particle size) analytical column was used as stationary phase, and a mixture of acetonitrile/water was used as the eluent working in gradient mode for the analysis of Br-NB and NB (10 to 70% acetonitrile) or isocratic for the analysis of I-NB (55% acetonitrile) and F-NB (60% acetonitrile), at a flow rate of 1 mL x min^{-1}. The chromatograms were analyzed at 254 nm.

Redox potential measurements

The redox potentials of the X-NB derivatives and the employed amines were determined using a 1 mM solution of the substrates together with 0.1 M TBA in acetonitrile, at room temperature and applying a scan rate of 0.1 V x s^{-1}. The values for the X-NB series were calculated as the average between the maximum and minimum of the cyclic potential scan curves. The values for the irreversible redox reactions of the amines correspond to the maximum obtained in the voltammograms. The data obtained vs Ag/AgCl (saturated KCl) were converted into redox potential values vs SCE (E (vs SCE, in V) = E (vs Ag/AgCl, in V) - 0.045).

Steady-state and time-resolved quenching of Ru(bpy)$_3$$^{2+}$ luminescence

　　　　　　　　　　　　　　　　ARTICLE

Deaerated solutions of $Ru(bpy)_3^{2+}$ (1 x 10^{-5} M) in a 4:1 mixture of acetonitrile-water (A_{460nm} = 0.14) were employed in the steady-state and time-resolved luminescence experiments. Stock solutions were kept in ice-baths and the temperature of the lab was also kept at 15 ºC. Quenching experiments were performed by adding increasing concentrations of X-NB or amines (in the range of 10^{-3} M) to the $Ru(bpy)_3^{2+}$ solutions. The steady-state and time-resolved luminescence traces of $Ru(bpy)_3^{2+}$ were recorded upon addition of the derivatives, and the obtained data used to determine the static and dynamic quenching rate constants applying the Stern-Volmer equations. The excitation spectrum of $Ru(bpy)_3^{2+}$ was recorded (from 250 to 600 nm) upon fixing the excitation wavelength at the emission maximum: 610 nm.

Kinetics of X-NB photoreduction monitored by HPLC

Deaerated solutions containing 1.5 x 10^{-4} mol of the nitrobenzene derivative (X-NB), 10% mol of $Ru(bpy)_3^{2+}$, DIPEA (*ca.* 10 eq) and isopropanol (*ca.* 90 eq) in acetonitrile-water (4:1) were placed in a Pyrex glass flask (total volume of 15 mL). The system was irradiated under stirring using the above described photoreactor. Special attention was made to keep the temperature of the reaction at *ca.* 15 ºC. With this aim the irradiation room was also kept at that temperature, a fan was used to dissipate the heat released by the LEDs and the reaction mixture was partially immersed in a cold-bath (2 cm height) that was regularly changed. The extent of the photoreduction was monitored upon extraction of an aliquot (40 μL) that was then diluted in 1 mL of acetonitrile-water (4:1) and injected (50 μL) in the HPLC system.

Results and discussion

Firstly, thermodynamic data were obtained from the redox potential measurements, and the free energy changes of the processes potentially involving excited states were estimated. Next, kinetic information was obtained from the dynamic behavior of the excited state lifetime of $Ru(bpy)_3^{2+}$ in the presence of the X-NB derivatives or the amines. Then, the photoredox processes were optimized for Br-NB and subsequently extended to the other three *p*-halonitrobenzenes (X-NB), including analysis of the photoproducts. Finally, an overall analysis was done to correlate the thermodynamic and kinetic experimental data.[28]

Thermodynamic feasibility of the redox processes

Although electron transfer is assumed to be responsible for the recently observed visible-light mediated photoredox transformations, the excited state of a photocatalyst could, in principle, generate the desired reactive intermediates through an energy transfer mechanism.[29-30]

To evaluate such option, the reported value for the energy of the excited state of $Ru(bpy)_3^{2+}$, taken from the emission maximum, is considered to be 47-48 kcal x mol^{-1}.[8] Although it is difficult to find a consensus method to determine the energy of the lower excited state when multiple levels are to be considered, such as for organometallic complexes,[31-32]
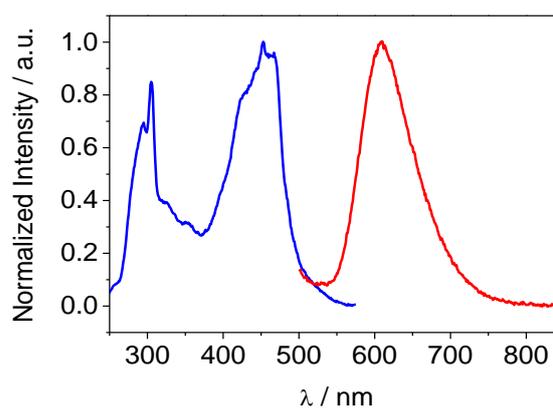

Fig. 2. Normalized emission and excitation spectra of $Ru(bpy)_3^{2+}$ in acetonitrile.

estimating the value from the emission maximum does not correspond to a widely accepted method. Nevertheless, a more appropriate photophysically-based protocol for determining the energy of the LUMO can be employed, based on thecross-point of the normalized emission and excitation spectra. For this purpose, such spectra of $Ru(bpy)_3^{2+}$ were recorded and normalized (Fig. 2). The energy that corresponds to the cross-point (λ = 525 nm, then E = 54.5 kcal x mol^{-1} = 2.36 eV) was established as the energy of the first excited state of $Ru(bpy)_3^{2+}$. This new value is consistent with thermodynamic estimations that otherwise would have resulted in endergonic PET processes through either cycle. In this particular case, by comparing the UV-visible spectra of $Ru(bpy)_3^{2+}$ and X-NB derivatives (data not shown), while the former absorbs in the visible up to 500 nm, the latter absorb at much shorter wavelength. Triplet energies for related nitrobenzene or chlorobenzene are 2.6 and 3.5 eV, respectively.[33] Therefore, although the energy of the triplet state cannot be directly estimated from the UV-visible spectra one can assume that it is higher than that of the excited state of $Ru(bpy)_3^{2+}$. Accordingly, energy transfer from the photocatalyst would be thermodynamically disfavored and can be safely discarded.

Nevertheless, it is widely accepted that $Ru(bpy)_3^{2+}$ can be involved in an oxidative and in a reductive quenching cycles (see Fig. 1). The thermodynamics of the two alternatives can be analyzed estimating the Gibbs free energy of the initial photoinduced electron transfer (PET) step using the formerly known as Rehm-Weller equation,[34-35] and from the Gibbs free energy for the subsequent thermal step. In our case, for the oxidative cycle the corresponding values of the two steps have been estimated according to eq. 1-2, while for the reductive cycle the values have been obtained from eq. 3-4.

$$\Delta G^o_{et}(eV) =$$
$$-[(E^o\,((X-NB)/(X-NB)^-) - E^o\,(Ru(bpy)_3^{3+}/Ru(bpy)_3^{2+})] - E(Ru(bpy)_3^{2+})^*\,(eq.\,1)$$

$$\Delta G^o(eV) =$$
$$-[E^o\,(Ru(bpy)_3^{3+}/Ru(bpy)_3^{2+}) - (E^o\,(R_3N^{\cdot+}/R_3N)]\;(eq.\,2)$$

$$\Delta G^o_{et}(eV) =$$
$$-[E^o\,(Ru(bpy)_3^{2+}/Ru(bpy)_3^{+}) - (E^o\,(R_3N^{\cdot+}/R_3N)] - E(Ru(bpy)_3^{2+})^*\,(eq.\,3)$$

$$\Delta G^o(eV) =$$
$$-[(E^o\,((X-NB)/(X-NB)^{\cdot-}) - E^o\,(Ru(bpy)_3^{2+}/Ru(bpy)_3^{+})]\;(eq.\,4)$$

Journal Name

ARTICLE

Table 1. Experimentally determined redox potentials of *p*-halonitrobenzene derivatives (X-NB) and amines, and thermodynamics of the two steps of the global redox process photocatalyzed by Ru(bpy)$_3$$^{2+}$ through the oxidative and reductive quenching cycles.

	Redox potentials			Oxidative quenching cycle		Reductive quenching cycle	
X	$E^o\,((X-NB)/(X-NB)^{\cdot-})$[a]	R_3N	$E^o\,(R_3N^{\cdot+}/R_3N)$[a]	ΔG_{et}^o [b]	ΔG^o [b]	ΔG_{et}^o [b]	ΔG^o [b]
H	-0.963	DIPEA	+0.972	-0.107	-0.318	-0.058	-0.367
F	-0.940	Aniline	+1.112	-0.130	-0.178	-0.082	-0.390
Cl	-0.872	TEA	+0.883	-0.198	-0.407	-0.147	-0.458
Br	-0.858			-0.212			-0.472
I	-0.848			-0.222			-0.482

Redox potentials are given in V *vs* SCE; b: energy values are given in eV

The reported redox potentials of Ru(bpy)$_3$$^{3+}$/Ru(bpy)$_3$$^{2+}$ and Ru(bpy)$_3$$^{2+}$/Ru(bpy)$_3$$^{+}$ are +1.29 V and -1.33 *vs* SCE, respectively.[8] Herein, the redox potentials of X-NB derivatives and amines such as DIPEA, aniline or trimethylamine (TEA) were determined under identical conditions using the above described equipment. The obtained values are shown in Table 1. As expected, the ability of X-NB to be reduced increases upon going down in the group of halogens. Using these values and the determined redox potentials, the ΔG of all the potentially involved processes were estimated (Table 1).

Based on the thermodynamic calculations reduction of nitrobenzene derivatives is exergonic and can in principle proceed through either the oxidative or through the reductive quenching cycle. It is worthy to notice the need for the new experimental determination of the energy of the first excited state of Ru(bpy)$_3$$^{2+}$, otherwise the PET processes through either cycle would have resulted endergonic.

Kinetic viability of the photoreduction of the p-halonitrobenzenes: steady-state and time resolved quenching of Ru(bpy)$_3$$^{2+}$ luminescence

In order to figure out the participation of the oxidative or reductive cycles in the overall redox reaction it is mandatory to check the kinetic viability of these processes within the time scale of the excited state of the Ru(bpy)$_3$$^{2+}$*.[36] Even more important is to compare the oxidative *versus* the reductive quenching of the (Ru(bpy)$_3$$^{2+}$)* by the X-NB derivatives and the amines, respectively, and discuss the relative quenching constants values and how they can determine the contribution of one or the other cycle in the overall process under the specific experimental conditions.

With this aim, the dynamics of its excited state upon addition of increasing concentrations of the X-NB derivatives was investigated by means of steady-state and time-resolved

luminescence. It has been reported that the emission intensity of Ru(bpy)$_3$$^{2+}$ and its lifetime decrease as the temperature increases.[37-38] For this reason, the photophysical experiments were performed under controlled temperature (15 ºC). Then, upon excitation at λ_{exc} = 460 nm, the intensity of the emission of [Ru(bpy)$_3$$^{2+}$]* decreased in the presence of increasing concentration of the X-NB derivatives keeping its characteristic shape (see Figure 3a for the case of Cl-NB as an example), thus indicating a potential participation of the excited state in an electron exchange process. To unequivocally demonstrate the participation of the excited state of Ru(bpy)$_3$$^{2+}$ in the photoreduction, time-resolved experiments were carried out upon increasing the concentration of the X-NB derivatives. As it can be seen in Figure 3b for the case of Cl-NB and in Figure 3c where the Stern-Volmer plots of all the X-NB derivatives are shown together, the lifetime of [Ru(bpy)$_3$$^{2+}$]* decreased with the concentration of X-NB from the initial value of 900 ns. Using the Stern-Volmer relationships for the static and dynamic quenchings (equations (5) and (6)), the K_{SV} and the k_q were determined for all the derivatives (Table 2). Table 2 shows the obtained results from the static (K_{SV}) and dynamic (k_q) quenching of Ru(bpy)$_3$$^{2+}$ luminescence by *p*-halonitrobenzenes.

$$I_o/I = 1 + K_{SV}[Q] \qquad \text{(eq. 5)}$$

$$\tau_o/\tau = 1 + k_q\tau_0[Q] \qquad \text{(eq. 6)}$$

The resulting values have been referred to the unsubstituted nitrobenzene for the sake of clarity. The obtained values for the nitro derivatives (X-NB) are in good agreement with the thermodynamic calculations. Moreover, the correlation found between the experimentally obtained kinetic constants and the calculated thermodynamic ΔG, shown in Figure 4, is in agreement with expectations from the Marcus theory.[39-40]
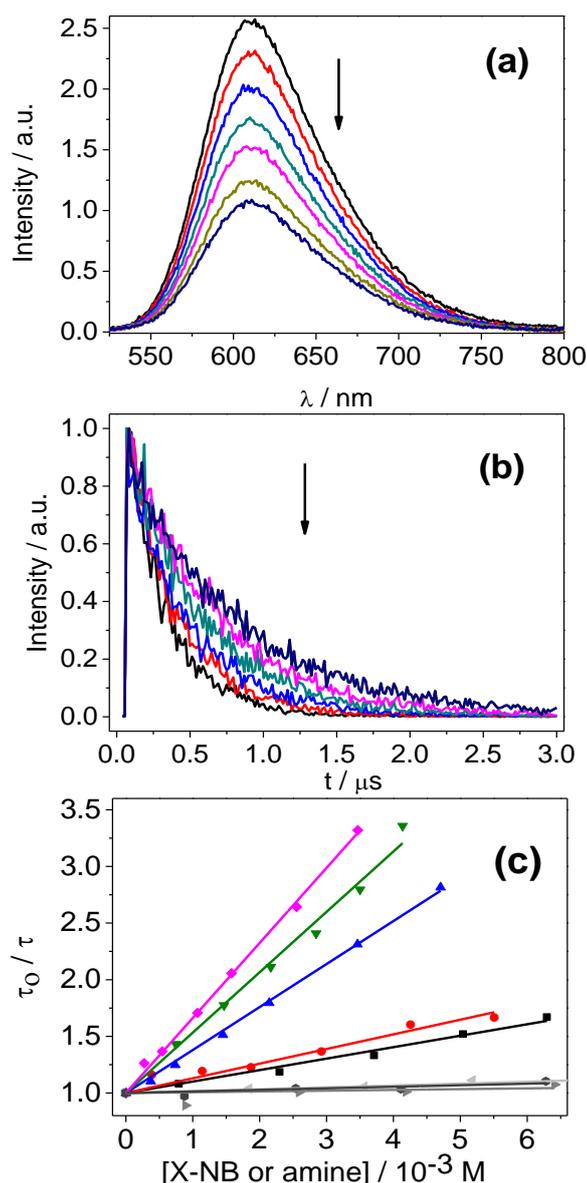
Fig 3. (a) Steady-state and **(b)** time-resolved quenching of the Ru(bpy)$_3^{2+}$ luminescence upon increasing concentrations of Cl-NB (up to $4.5 \cdot 10^{-3}$ M) as an example; **(c)** Stern-Volmer fittings for the time-resolved lumniscence quenching by I-NB (pink), Br-NB (green), Cl-NB (blue), F-NB (red), NB (black), DIPEA (light gray), aniline (grey) and TEA (dark grey).

Reductive quenching of excited Ru(bpy)$_3^{2+}$ by amines has been studied from the 1970s using laser-flash photolysis.[32, 41-43] However, the reported quenching rate constants for aliphatic amines are very low, in the order of 10^6 M^{-1}s^{-1} (k_q= 6.2 x 10^6 M^{-1}s^{-1} for DIPEA as example).[44] Accordingly, in our hands the Stern-Volmer plots obtained from the time-resolved data are shown in Figure 3c together with the ones found for the X-NB derivatives for comparison. Nevertheless, although the amines are able to quench the excited state to a certain extent, their efficiency compared to that of the X-NB derivatives is at least two orders of magnitude lower. Therefore, at the concentrations used in this work ([amine] is ten-fold that of the [X-NB]), quenching of [Ru(bpy)$_3^{2+}$]* happens mainly through the oxidative cycle (Fig. 5).

Thermodynamic estimations on the overall reduction of X-NB and oxidation of amines photocatalyzed by Ru(bpy)$_3^{2+}$ under visible light are compatible with both cycles. The key experiment to determine if the overall process involves the oxidative or reductive quenching cycles is the analysis of the relative efficiency of the two reactants in the quenching of [Ru(bpy)$_3^{2+}$]* at the concentrations used. If the excited state is more efficiently quenched by the amine it enters into the reductive cycle giving rise to Ru(bpy)$_3^+$, that subsequently reduces the X-NB. Conversely, if the excited state more efficiently reduces X-NB, it enters into the oxidative cycle giving rise to Ru(bpy)$_3^{3+}$, that subsequently oxidizes the amine. In our hands, reduction of X-NB is more efficient than oxidation of amines at the employed concentrations, thus supporting the involvement of the oxidative quenching cycle.

Examples of different scenarios can be found in literature in which the reductive catalytic cycle is claimed as the operating one;[26, 45-50] It could be assumed that the quenching constants of the two reactants are in the same order of magnitude and the ratio of concentrations favors the reductive cycle; however, no time-resolved kinetic analysis has been undertaken, and the proposed mechanism is based on the fact that the used amines are able to reduce [Ru(bpy)$_3^{2+}$]* and thus start the reductive quenching cycle.

Table 2. Obtained values for the Stern-Volmer (K$_{SV}$) and time-resolved quenching constants (k_q) for the reaction between the excited state of Ru(bpy)$_3^{2+}$ and the X-NB derivatives.

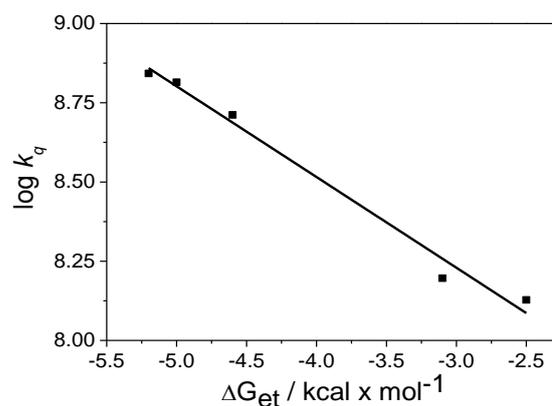| X	K$_{SV}$ / M^{-1}	K$_{SV}$ / K$_{SV}$ (NB)	k_q / 10^8 M^{-1} x s^{-1}	k_q / k_q (NB)
H	92.9	1.0	1.3	1.0
F	99.7	1.1	1.6	1.2
Cl	294.5	3.2	5.1	3.8
Br	395.3	4.3	6.5	4.9
I	531.9	5.7	7.0	5.2

Fig. 4. Correlation between $log\ k_q$ and ΔG_{et} for the reduction of the *p*-halonitrobenzene derivatives photocatalyzed by [Ru(bpy)$_3^{2+}$]*.

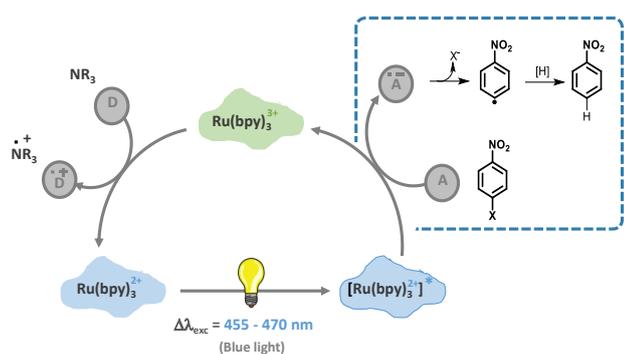**Fig. 5.** Photodehalogenation of *p*-halonitrobenzenes in the presence of sacrificial amines, catalyzed by Ru(bpy)$_3^{2+}$ under visible light, proceeding through its oxidative catalytic cycle.

Photodehalogenation of *p*-halonitrobenzenes in the presence of Ru(bpy)$_3^{2+}$

As a final step, the extent of the dehalogenation of the X-NB derivatives and the nature of the obtained photoproducts was investigated.

To set-up the reaction, DIPEA was chosen among the different amines as sacrificial donor.[26-27] Secondly, among the reported hydrogen donors needed for the last step, the reported formic acid and Hantzsch ester were examined.[26, 51-53] However, in our hands, a considerable amount of unstable by-products and a very low concentration of nitrobenzene (NB, the common dehalogenated product for all the X-NB derivatives) were found. Nevertheless, using a simpler hydrogen donor, such as isopropanol in large excess, higher yields of NB were obtained. In the optimized reaction conditions, deaerated solutions containing 1.5 x 10^{-4} mol of the nitrobenzene derivative (X-NB), 10% mol of Ru(bpy)$_3^{2+}$, DIPEA (*ca.* 10 eq) and isopropanol (*ca.* 90 eq) in acetonitrile-water (4:1) were placed in a Pyrex glass flask (total volume of 15 mL) and irradiated (λ_{irr} = 460 nm) under stirring using the photoreactor shown in Fig. 6 bottom left. The results obtained for I-NB under these reaction conditions are shown in Fig. 6 top and bottom right. Longer irradiation times were required for the other X-NB (data not shown). Initially, different polar solvents such as DMF were examined, nevertheless the best results were found using acetonitrile-water (4:1). Control experiments showed that in the absence of the photocatalyst or in darkness only trace amounts of NB after long irradiation were obtained.

Conclusions

Fast kinetic data obtained from time-resolved emission spectroscopy, have proven valuable to gain a deeper understanding of the mechanism involved in the visible-light photocatalytic reduction of halonitrobenzene derivatives mediated by Ru(bpy)$_3$Cl$_2$. The obtained kinetic rate constants correlate well with thermodynamic estimations on the free energy changes associated with the key electron transfer step.
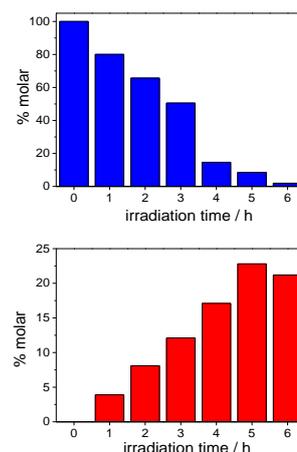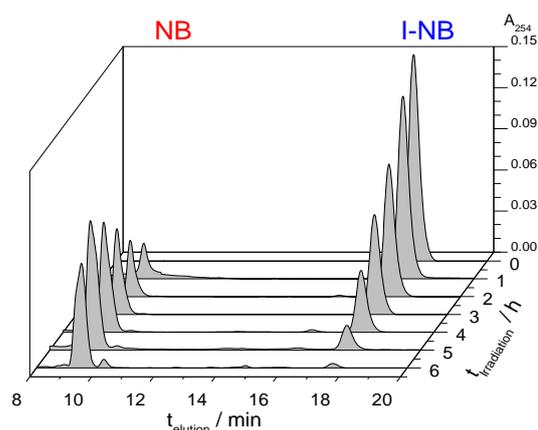

Fig. 6. (top) Chromatogram of photoreaction of I-NB in presence of 10% mol of Ru(bpy)$_3^{2+}$ and an excess of DIPEA and *i*-PrOH; **(bottom)** experimental set-up, percentage of remaining I-NB and formation of NB under the optimized reaction conditions.

Even more important, unequivocal support for the participation of the oxidative quenching cycle under the experimental conditions employed has been obtained from time-resolved kinetic experiments.

Deep knowledge on the involved mechanism of such photoredox reaction represents a strong scientific pillar to design improved technological applications.

Acknowledgements

Notes and references

1 D. Ravelli, D. Dondi, M. Fagnoni and A. Albini, *Chem. Soc. Rev.* 2009, *38*, 1999.

2 G. Palmisano, V. Augugliaro, M. Pagliaro and L. Palmisano, *Chem. Commun.* 2007, 3425.

3 M. L. Marin, L. Santos-Juanes, A. Arques, A. M. Amat and M. A. Miranda, *Chem. Rev.* 2012, *112*, 1710.

4 R. Martinez-Haya, M. H. Barecka, P. Miro, M. L. Marin and M. A. Miranda, *Appl. Catal. B* 2015, *179*, 433.

5 P. Miró, A. Arques, A. M. Amat, M. L. Marin and M. A. Miranda, *Appl. Catal. B* 2013, *140–141*, 412.

6 L. Huang, Y. Shen, W. Dong, R. Zhang, J. Zhang and H. Hou, *J. Hazard. Mater.* 2008, *151*, 323.

7 J. W. Tucker and C. R. J. Stephenson, *J. Org. Chem.* 2012, *77*, 1617.

8 C. K. Prier, D. A. Rankic and D. W. C. MacMillan, *Chem. Rev.* 2013, *113*, 5322.

9 J. M. R. Narayanam and C. R. J. Stephenson, *Chem. Soc. Rev.* 2011, *40*, 102.

10 Y. M. Xi, H. Yi and A. W. Lei, *Org. Biomol. Chem.* 2013, *11*, 2387.

11 D. Alpers, M. Gallhof, J. Witt, F. Hoffmann and M. Brasholz, *Angew. Chem., Int. Ed.* 2017, *56*, 1402.

12 B. König, *Eur. J. Org. Chem.* 2017, *2017*, 1979.

13 F. Teply, *Collect. Czech. Chem. Commun.* 2011, *76*, 859.

14 G. Bergonzini, C. S. Schindler, C.-J. Wallentin, E. N. Jacobsen and C. R. J. Stephenson, *Chem. Sci.* 2014, *5*, 112.

15 D. A. Nicewicz and D. W. C. MacMillan, *Science* 2008, *322*, 77.

16 A. McNally, C. K. Prier and D. W. C. MacMillan, *Science* 2011, *334*, 1114.

17 K.-H. He, F.-F. Tan, C.-Z. Zhou, G.-J. Zhou, X.-L. Yang and Y. Li, *Angew. Chem., Int. Ed.* 2017, *56*, 3080.

18 L. Ruiz Espelt, I. S. McPherson, E. M. Wiensch and T. P. Yoon, *J. Am. Chem. Soc.* 2015, *137*, 2452.

19 D. A. DiRocco and T. Rovis, *J. Am. Chem. Soc.* 2012, *134*, 8094.

20 E. R. Welin, A. A. Warkentin, J. C. Conrad and D. W. C. MacMillan, *Angew. Chem., Int. Ed.* 2015, *54*, 9668.

21 M. T. Pirnot, D. A. Rankic, D. B. C. Martin and D. W. C. MacMillan, *Science* 2013, *339*, 1593.

22 J. W. Beatty and C. R. J. Stephenson, *Acc. Chem. Res.* 2015, *48*, 1474.

23 D. Rosner and G. Markowitz, *Environ. Res.* 2013, *120*, 126.

24 D. Limones-Herrero, R. Perez-Ruiz, M. C. Jimenez and M. A. Miranda, *Org. Lett.* 2013, *15*, 1314.

25 F. Alonso, I. P. Beletskaya and M. Yus, *Chem. Rev.* 2002, *102*, 4009.

26 J. M. R. Narayanam, J. W. Tucker and C. R. J. Stephenson, *J. Am. Chem. Soc.* 2009, *131*, 8756.

27 J. D. Nguyen, E. M. D'Amato, J. M. R. Narayanam and C. R. J. Stephenson, *Nat. Chem.* 2012, *4*, 854.

28 R. Martinez-Haya, M. A. Miranda and M. L. Marin, *Eur. J. Org. Chem.* 2017, *2017*, 2164.

29 E. R. Welin, C. Le, D. M. Arias-Rotondo, J. K. McCusker and D. W. C. MacMillan, *Science* 2017, *355*, 380.

30 T. R. Blum, Z. D. Miller, D. M. Bates, I. A. Guzei and T. P. Yoon, *Science* 2016, *354*, 1391.

31 K. Kalyanasundaram, *Coord. Chem. Rev.* 1982, *46*, 159.

32 A. Juris, V. Balzani, F. Barigelletti, S. Campagna, P. Belser and A. von Zelewsky, *Coord. Chem. Rev.* 1988, *84*, 85.

33 S. L. Murov, I. Carmichael and G. L. Hug, *Handbook of Photochemistry, 2nd ed.*, Marcel Dekker, New York, **2009**, p.

34 D. Rehm and A. Weller, *Isr. J. Chem.* 1970, *8*, 259.

35 S. E. Braslavsky, A. U. Acuna, W. Adam, F. Amat, D. Armesto, T. D. Z. Atvars, A. Bard, E. Bill, L. O. Bjoern, C. Bohne, J. Bolton, R. Bonneau, H. Bouas-Laurent, A. M. Braun, R. Dale, K. Dill, D. Doepp, H. Duerr, M. A. Fox, T. Gandolfi, Z. R. Grabowski, A. Griesbeck, A. Kutateladze, M. Litter, J. Lorimer, J. Mattay, J. Michl, R. J. D. Miller, L. Moggi, S. Monti, S. Nonell, P. Ogilby, G. Olbrich, E. Oliveros, M. Olivucci, G. Orellana, V. Prokorenko, K. R. Naqvi, W. Rettig, A. Rizzi, R. A. Rossi, R. E. San, F. Scandola, S. Schneider, E. W. Thulstrup, B. Valeur, J. Verhoeven, J. Warman, R. Weiss, J. Wirz and K. Zachariasse, *Pure Appl. Chem.* 2007, *79*, 293.

36 S. P. Pitre, C. D. McTiernan and J. C. Scaiano, *Acc. Chem. Res.* 2016, *49*, 1320.

37 K. J. Morris, M. S. Roach, W. Xu, J. N. Demas and B. A. DeGraff, *Anal. Chem.* 2007, *79*, 9310.

38 J. V. Caspar and T. J. Meyer, *J. Am. Chem. Soc.* 1983, *105*, 5583.

39 R. A. Marcus and H. Eyring, *Annu. Rev. Phys. Chem.* 1964, *15*, 155.

40 M. A. Miranda, M. A. Izquierdo and R. Pérez-Ruiz, *J. Phys. Chem. A* 2003, *107*, 2478.

41 R. Ballardini, G. Varani, M. T. Indelli, F. Scandola and V. Balzani, *J. Am. Chem. Soc.* 1978, *100*, 7219.

42 G. S. Laurence and V. Balzani, *Inorg. Chem.* 1974, *13*, 2976.

43 C. R. Rivarola, S. G. Bertolotti and C. M. Previtali, *Photochem. Photobiol.* 2006, *82*, 213.

44 S. P. Pitre, C. D. McTiernan, H. Ismaili and J. C. Scaiano, *J. Am. Chem. Soc.* 2013, *135*, 13286.

45 X. Li, Z. Hao, F. Zhang and H. Li, *ACS Applied Materials & Interfaces* 2016, *8*, 12141.

46 R. Ananthakrishnan and S. Gazi, *Catal. Sci. Technol.* 2012, *2*, 1463.

47 S. Gazi and R. Ananthakrishnan, *Appl. Catal. B* 2011, *105*, 317.

48 J. Liu, Q. Liu, H. Yi, C. Qin, R. Bai, X. Qi, Y. Lan and A. Lei, *Angew. Chem. Int. Ed.* 2014, *53*, 502.

49 H. Wang, Q. Lu, C.-W. Chiang, Y. Luo, J. Zhou, G. Wang and A. Lei, *Angew. Chem. Int. Ed.* 2017, *56*, 595.

50 H. Yi, X. Zhang, C. Qin, Z. Liao, J. Liu and A. Lei, *Adv. Synth. Catal.* 2014, *356*, 2873.

51 Y. Chen, A. S. Kamlet, J. B. Steinman and D. R. Liu, *Nat. Chem.* 2011, *3*, 146.

52 M.-H. Larraufie, R. Pellet, L. Fensterbank, J.-P. Goddard, E. Lacote, M. Malacria and C. Ollivier, *Angew. Chem., Int. Ed.* 2011, *50*, 4463.

53 R. S. Andrews, J. J. Becker and M. R. Gagne, *Angew. Chem., Int. Ed.* 2010, *49*, 7274.